

Orthogonal Structure Search for Efficient Causal Discovery from Observational Data

Anant Raj¹ Luigi Gresele¹ Michel Besserve¹ Bernhard Schölkopf¹ Stefan Bauer¹

Abstract

The problem of inferring the direct causal parents of a response variable among a large set of explanatory variables is of high practical importance in many disciplines. Recent work exploits stability of regression coefficients or invariance properties of models across different experimental conditions for reconstructing the full causal graph. These approaches generally do not scale well with the number of the explanatory variables and are difficult to extend to nonlinear relationships. Contrary to existing work, we propose an approach which even works for observational data alone, while still offering theoretical guarantees including the case of partially nonlinear relationships. Our algorithm requires only one estimation for each variable and in our experiments we apply our causal discovery algorithm even to large graphs, demonstrating significant improvements compared to well established approaches.

1. Introduction

Identifying causal relationships is a core problem of science. While randomized controlled studies are considered as the gold standard, the approach can in many cases be ruled out by financial or ethical concerns (Spirtes et al., 2000; Pearl, 2009; Peters et al., 2017).

To identify causal structure, recently proposed methods aim to exploit invariance or stability when data from different experimental settings is available (Peters et al., 2016; Ghassemi et al., 2017; Pfister et al., 2018b;a).

Formally, this reads

$$Y^e | \{X_{|S^*}^e = x\} \stackrel{d}{=} Y^f | \{X_{|S^*}^f = x\}, \quad (1)$$

and implies that the conditional distribution of the response given the causal parents in the set S^* is the same across all

¹Max Planck Institute for Intelligent Systems, Tübingen, Germany. Correspondence to: Anant Raj <anant.raj@tuebingen.mpg.de>.

instances e, f of environments $e, f \in \mathcal{E}$. For this assumption to hold, it is required that all variables are observed and that the interventions which define the environments do not have a direct effect on the response Y . A more formal discussion is provided in Section 2.

However most state of the art methods suffer from scalability problems since they scan all potential subsets of variables and test whether the conditional distribution of Y given a subset of variables is invariant across all environments (Peters et al., 2016). This search is hence exponential in the number of covariates; the methods, while maintaining appealing theoretical guarantees, are thus already computationally hard for graphs of ten variables, and get infeasible for larger graphs, unless one resorts to heuristic procedures. An efficient inference procedure, especially for observational data alone, has so far been missing (Heinze-Deml et al., 2018) and motivates the present work. Here we investigate an important sub-problem of the general causal discovery problem, specifically that of discovering direct causes of Y among a high-dimensional vector of variables $X = (X_1, X_2, \dots, X_d)$. We consider the problem where we want to infer the direct causes $S^* \subseteq \{1, \dots, d\}$ among the covariates X_1, \dots, X_d , rather than the full causal graph structure.

CONTRIBUTIONS:

Building on procedures for debiased estimation of true causal effects in the presence of confounding (Chernozhukov et al., 2016; Javanmard & Montanari, 2015), we develop a novel method which can discover the true causal parents with a computational complexity in $\mathcal{O}(d)$, largely outperforming state-of-the-art rate of $\mathcal{O}(2^d)$, while requiring a linearity assumption only for the influence of the direct causal parents and allowing for nonlinear interactions among the covariates. Contrary to existing work, our approach likewise works, when only observational data is available (Nichols, 2008; Maathuis et al., 2010).

OUTLINE:

In Section 2, we review current state-of-the-art approaches for identifying direct parents of a target variable Y . In Section 3 we describe our approach and give a theoretical

identifiability result for a partially nonlinear model. In Section 4 we confirm in extensive experiments the scaling of our algorithm and demonstrate its empirical performance for causal discovery. We also illustrate and give arguments for an extension in the presence of hidden confounders, and conclude with Section 5.

2. Related work

Inferring causal relationships from observational data is a challenging task. Most of the existing approaches require strong assumptions, such as faithfulness (Spirtes et al., 2000; Pearl, 2009). Classical approaches along these lines include the PC-algorithm (Spirtes et al., 2000), which can only reconstruct the network up to a Markov equivalence class. Another approach is to restrict the class of interactions among the covariates and the functional form of the signal-noise mixing (typically considered additive) or the distribution (e.g., non-Gaussianity) to achieve identifiability (see Hoyer et al. (2009); Peters et al. (2014)); this includes linear approaches like LiNGAM (Shimizu et al., 2006) and nonlinear generalizations with additive noise (Peters et al., 2011). For a recent review of the empirical performance of structure learning algorithms, we refer to Heinze-Deml et al. (2018).

2.1. Invariant Causal Prediction

Invariant Causal Prediction (Peters et al., 2016) proposes a method to find the causal parents of a target variable without the faithfulness assumption or restrictions on the form of the noise distribution. The main idea is to exploit invariance of the prediction when based exclusively on causal parents of the target variable i.e. the causal set of variables X^{S^*} and the associated causal coefficients β^* are required to be stable across different experimental settings:

Assumption 1. *There exists a vector β^* of causal coefficients such that*

$$\forall e \in \mathcal{E} : Y^e = X^e \beta^* + \varepsilon^e, \quad \varepsilon^e \sim F_e$$

$S^* = \{j, \beta_j^* \neq 0\}$ causal predictors

ε^e independent of X_S^* ,

where the noise distribution F_e is the same for all environments e , with mean zero and finite variance.

Assuming such invariance, an algorithm can go through the power set of the covariates, iteratively selecting subsets of variables; building predictive models based solely on those; and rejecting or accepting a subset depending on how invariant its prediction is across different environments, e.g., by checking whether the distribution of the residuals changes.

For each subset $S \subseteq \{1, \dots, d\}$ of explanatory variables,

the algorithm tests whether the invariance (1) holds true, and returns

$$\tilde{S} := \bigcap_{S \text{ fulfills (1)}} S. \quad (2)$$

Due to Assumption 1, \tilde{S} contains all variables from S^* . More heterogeneity in the experiments will help remove spurious variables whose conditionals may be stable in some experiments. One key contribution of Peters et al. (2016, Theorem 1) is that with large probability the inferred set is a subset of the true set of causal predictors.

The advantage of the approach is that it provides sound confidence intervals without relying on identifiability assumptions such as faithfulness (Spirtes et al., 2000), and that the interventions do not have to be specified, i.e., it is not required that the variables which are intervened on are explicitly indicated, as long as they do not include the target variable Y itself or change the distribution of F_e .

There are, however, several drawbacks to the method. The method can not be applied to observational data, interventions which do not affect the target variable may be difficult to design in practice, interactions among the covariates may be non-linear, and feedback loops inherently represented in real-world data are likewise difficult to handle (e.g. Mooij et al., 2011). Moreover, the intersection in (2) often returns the empty set and is too conservative for many practical applications (Rothenhäusler et al., 2018).

While there have been attempts to extend the method to include the case of hidden variables (Christiansen & Peters, 2018) (H-ICP), nonlinear relationships (Heinze-Deml et al., 2018) (N-ICP), or observational data where environments are defined with respect to time (Pfister et al., 2018b) (S-ICP), one significant drawback is the computational infeasibility of the method in the case of high-dimensional data. For maintaining its theoretical guarantees, all versions of the ICP algorithm iterate through the power set of the covariates, which for d variables grows as 2^d .

2.2. Regression Invariance

While Peters et al. (2016) focus on the invariance of the residual, Ghassami et al. (2017) use the stability of the regression coefficient. They introduce the notion of I -distinguishability. Given a set of variables I , two graphs are said to be I -distinguishable if, given that the variables in the I set change their exogenous noise distributions between two environments, the regression coefficients change, $R(G_1, I) \neq R(G_2, I)$. Exploiting this, the authors propose a method that achieves a lower computational complexity than ICP. However, some structures remain unidentifiable in the absence of proper interventions. Figure 1 shows a graph which is identifiable when $I = \{X_2\}$, but not identifiable when $I = \{X_1\}$.

Unlike both Peters et al. (2016) and Ghassami et al. (2017), we prove in Lemma 2 that our approach correctly identifies the direct causal parents of X_3 even if only observational data is available.

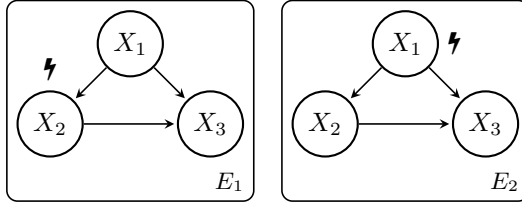


Figure 1. From (Ghassami et al., 2017, Figure 2): the structure is I -indistinguishable for $I = \{X_2\}$, but it is not for $I = \{X_1\}$. ⚡ stands for an intervention on the variables which characterize the environment E .

2.3. Double Machine Learning

Our method builds on recent research on Double Machine Learning, an estimation procedure for true causal effects in settings where confounding is present (Chernozhukov et al., 2016). Consider the partially linear regression model

$$\begin{aligned} Y &= D\theta_0 + g_0(X) + U, \quad \mathbb{E}[U|X, D] = 0 \\ D &= m_0(X) + V, \quad \mathbb{E}[V|X] = 0, \end{aligned} \quad (3)$$

where Y is the outcome variable, and D a “policy” variable whose effect on Y we seek to identify. X consists of *confounding* or *control* variables which affect the outcome Y and the policy variable D , and U, V are disturbances. θ_0 is the main regression coefficient that we would like to infer, interpreted as the direct causal effect of D on the outcome Y . The confounding factors X affect the policy variable D via the function $m_0(X)$, and the outcome variable via the function $g_0(X)$. Both m_0 and g_0 may be nonlinear functions of X , however the effect of the policy variable on the outcome variable is restricted to be linear.

Regularization Bias: A naive ML estimator of θ_0 can be obtained by an alternating estimation approach: first estimate \hat{g}_0 and then estimate $\hat{\theta}_0$. This would yield

$$\hat{\theta}_0 = \left(\frac{1}{n} \sum_{i \in I} D_i^2 \right)^{-1} \frac{1}{n} \sum_{i \in I} D_i (Y_i - \hat{g}_0(X_i)).$$

The bias induced in learning \hat{g}_0 will generally prevent or slow down the convergence of $\hat{\theta}_0$ to θ_0 (Chernozhukov et al., 2016). To heuristically illustrate the impact of the bias in learning g_0 , the following decomposition of the estimation

error in estimating the parameter $\hat{\theta}_0$ can be done:

$$\begin{aligned} \sqrt{n} (\hat{\theta}_0 - \theta_0) &= \underbrace{\left(\frac{1}{n} \sum_{i \in I} D_i^2 \right)^{-1} \frac{1}{n} \sum_{i \in I} D_i U_i}_{:=a} \\ &\quad + \underbrace{\left(\frac{1}{n} \sum_{i \in I} D_i^2 \right)^{-1} \frac{1}{n} \sum_{i \in I} D_i (g_0(X_i) - \hat{g}_0(X_i))}_{:=b} \end{aligned} \quad (4)$$

It is now easier to see that while the term ‘a’ has a controlled behaviour, the effect of the regularization bias kicks in the term ‘b’ and diverges in general because of the fact that \hat{g}_0 is a biased estimator of g_0 .

Overcoming Regularization Biases using Orthogonalization: To overcome the problem described above, Chernozhukov et al. (2016) introduce an orthogonal regressor V which directly partials out the effect of X from D , i.e., $V = D - m_0(X)$. More specifically, we obtain $\hat{V} = D - \hat{m}_0(X)$ where \hat{m}_0 is an ML estimator of m_0 obtained using an auxiliary sample of observations. After partialling the effect of X out from D and obtaining a preliminary estimate of g_0 from the auxiliary sample as before, we may formulate the following “debiased” machine learning estimator for θ_0 using the main sample of observations:

$$\check{\theta}_0 = \left(\frac{1}{n} \sum_{i \in I} \hat{V}_i D_i \right)^{-1} \frac{1}{n} \sum_{i \in I} \hat{V}_i (Y_i - \hat{g}_0(X_i)) \quad (5)$$

The estimation error for the estimator can be decomposed similar to the decomposition done in equation (4) which further is shown to be an unbiased estimator of the true parameter θ_0 in (Chernozhukov et al., 2016). The Neyman orthogonality condition (Neyman, 1979) is at the heart of the estimator (5) which we briefly discuss now.

Neyman Orthogonality Condition: The traditional estimator of θ_0 can be simply obtained by finding the zero of the empirical average of the score function which is actually solving for the first order optimality condition of the objective function. For the partially linear regression model given in equation (3), the score function ψ is: $\psi(W; \theta, g) = D^\top (Y - D\theta - g(X))$. However, we can see that the estimation is sensitive to the bias in the estimation of the function g .

Neyman proposed an orthogonalization approach to get the estimate for θ which is more robust to the biases in the estimation of nuisance parameter. For a moment if we assume that the true nuisance parameter is η_0 (which represents m_0 and g_0 in equation (3)) and the estimated one is denoted by $\hat{\eta}_0$. Then the orthogonalized “score” function ψ should satisfy the property that the Gateaux derivative

operator with respect to η vanishes when evaluated at the true parameter values:

$$\partial_\eta \mathbb{E}\psi(W; \theta_0, \eta_0)[\eta - \eta_0] = 0 \quad (6)$$

The condition given in the equation (6) is known as ‘‘Neyman orthogonality’’ and ψ is referred as Neyman orthogonal score function (Neyman, 1979). There are many possible ways discussed in the paper (Chernozhukov et al., 2016) to get the Neyman orthogonal score.

The estimator discussed in the equation (5) can simply be derived from the Neyman orthogonality condition.

3. Method

As discussed in the previous section, given a fixed set of policy variables D and control variables X , an unbiased estimator of the parameter θ_0 in equation (3) can be obtained via the orthogonalization described in the previous section. However, the distinction between policy variable and confounding variables is not always known in advance, which motivates us to consider a setting of causal discovery. The aim of this section is to describe our approach to identify the direct causal parents of the outcome variable Y . To this end, we consider a set of variables $Z = \{X_1, X_2, \dots, X_p\}$ which includes direct causes as well as other variables.

Assumptions: Throughout the paper, we follow the approach of double ML and assume that the relationship between outcome variable and direct causal parents of the outcome variable is linear. The relationship among other variables can be nonlinear. We also assume that the outcome variable has no children and believe that many real world applications could fit into this picture, e.g. the relationship genotype-phenotype.

Before going into the details of the proposed algorithm, we would first discuss the main idea behind our proposed approach and then later we provide a pseudo-code for our proposed method in Algorithm 1. For intuition, let us first assume that all interactions are linear and each variable has its own independent noise component. The idea is to do a one-vs-rest split for each variable in turn, and try to estimate the link between that variable and the outcome variable. Referring to the Double ML terminology in section 2.3, we can describe our estimation algorithm as follows:

1. Select one of the variables $X_i \equiv D$, of which we want to estimate the (hypothetical) linear causal effect θ on Y ;
2. Set all of the other variables $X_{\setminus i}$ as the set of possible confounders $X_{\setminus i} \equiv X$ in equation (3);
3. Using sample splitting estimate the parameter θ i.e. the causal effect of X_i on Y .

4. If the variable X_i is not a causal parent, the distribution of the estimated parameters will be a Gaussian centered around zero.

Using a statistical test (in the experiments we use a z-test), we can then decide to accept the variable as a causal parent or reject it depending on the outcome. We then iteratively repeat the procedure on each of the variables until completion.

Although we assume that there are no children of the outcome variable Y , we note that there are methods in the literature which can be used to separate children of the outcome variable from the rest of the variables in case there exists children for the output variable. Since our method should not be heavily affected by weak intervention on the outcome variable, such interventions could possibly be used to remove the children node of the outcome variable by directly intervening on the outcome variable and observing the effects. Otherwise, separating children from a target node y can be done in constant cost under the assumption of an additive noise model with an asymptotically consistent algorithm (Mooij et al., 2009).

We first provide a result for the DAG given in Figure 1. We assume that X_3 is the output variable which we denote here and in the rest of the paper with Y . We have the following linear structural equation model:

$$\begin{aligned} Y &\equiv X_3 := a_{13}X_1 + a_{23}X_2 + \varepsilon_3 \\ X_2 &:= a_{12}X_1 + \varepsilon_2 \\ X_1 &:= \varepsilon_1 \end{aligned} \quad (7)$$

Example 2. Let us consider the DAG given in Figure 1 whose structure equation model is given in (7). If ε_1 , ε_2 and ε_3 are independent uncorrelated noise terms, then Algorithm 1 will recover the coefficients a_{13} and a_{23} .

Proof. The derivation is given in Appendix A. \square

The result given in Example 2 provides intuition in understanding the method. In the linear case, the method not only works in the causal direction, but also in the anti-causal direction. However the next result we provide comes from the Neyman (1979) orthogonality condition and works for more general cases.

3.1. Influence of the interactions between parents

In the following we use a generic example shown in Figure 2 to illustrate the role of interactions between the covariates on the proposed causal discovery algorithm.

Lemma 3. Assume the partially linear Gaussian model of Fig. 2, denote $\mathbf{Z} = [\mathbf{Z}_1^\top, \mathbf{Z}_2^\top]^\top$ the control variables, $\gamma = (\gamma_1, \gamma_1, \gamma_{12})$ the parameter vector of the (possibly

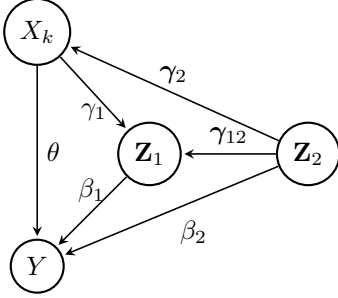


Figure 2. Generic example of identification of a causal effect θ in the presence causal and anticausal interactions between the causal predictor and other putative parents, and possibly arbitrary nonlinear and non-invertible assignments for all nodes except Y (see Lemma 3).

non-linear) assignments between putative parents of Y , and $\beta = (\beta_1, \beta_2)$ the vector of causal coefficients for encoding linear effects of \mathbf{Z} on outcome Y . Then, independently from the γ parameters and of the functional form of the associated assignments between parents of Y , the score

$$\psi(\mathbf{W}; \theta, \beta) = (Y - X_k \theta - \mathbf{Z}^\top \beta)(X_k - \mathbf{r}_{XZ} \mathbf{Z}), \quad (8)$$

with $\mathbf{r}_{XZ} = \mathbb{E}[X_k \mathbf{Z}^\top] \mathbb{E}[\mathbf{Z} \mathbf{Z}^\top]^{-1}$, follows the Neyman orthogonality condition for the estimation of θ with nuisance parameters $\eta = (\beta, \gamma)$ which reads

$$\mathbb{E}[(Y - X_k \theta - \mathbf{Z}^\top \beta)(X_k - \mathbb{E}[X_k \mathbf{Z}^\top] \mathbb{E}[\mathbf{Z} \mathbf{Z}^\top]^{-1} \mathbf{Z})] = 0. \quad (9)$$

Proof. The proof is given in the Appendix. \square

The result discussed in Lemma 3 is not directly intuitive. In simple words, there are two takeaways from Lemma 3: (i) the orthogonality condition remains invariant irrespective of the causal direction between X_k and Z , and (ii) the second term in equation 9 suggests to use a linear estimator for modeling all the relations, given that the relation between \mathbf{Z} and Y is linear.

To generate more intuition, we provide a few examples. Let us go back again to the three variable interaction given in Figure 1 assuming the following structural equation model:

$$\begin{aligned} Y &\equiv X_3 := a_1 X_1 + a_2 X_2 + \varepsilon_3 \\ X_2 &:= f(X_1) + \varepsilon_2 \\ X_1 &:= \varepsilon_1, \end{aligned} \quad (10)$$

where f is a nonlinear function and $\varepsilon_1, \varepsilon_2$ and ε_3 are zero mean Gaussian noises.

- Consider the case when $f(x) = x^2$. The goal is to estimate the parameter a_1 which we call \hat{a}_1 . We follow

the standard double ML procedure assuming policy variable X_1 and control X_2 , although the ground truth causal dependency $X_1 \rightarrow X_2$ in contradiction with such setting (see equation (3)). The estimate of a_2 following the double ML procedure, which we call $\hat{a}_2 = \frac{\mathbb{E}[X_2 Y]}{\mathbb{E}[X_2^2]} = a_2 + a_1 \frac{\mathbb{E}[X_1 X_2]}{\mathbb{E}[X_2^2]}$. Similarly, we want to estimate $X_1 = \alpha X_2 + \eta$ from which we get, $\alpha = \frac{\mathbb{E}[X_1 X_2]}{\mathbb{E}[X_2^2]}$. It is easy to see that $\mathbb{E}[X_1 X_2] = \mathbb{E}[X_1^3] = 0$. Hence, $\alpha = 0$ and it is easy to see $\hat{a}_1 = a_1$.

- Consider now the more general case where f is any nonlinear function. As in the previously discussed example, the goal is to estimate a_1 . We have $\hat{a}_2 = \frac{\mathbb{E}[X_2 Y]}{\mathbb{E}[X_2^2]} = a_2 + a_1 \frac{\mathbb{E}[X_1 X_2]}{\mathbb{E}[X_2^2]}$. Similarly, $\alpha = \frac{\mathbb{E}[X_1 X_2]}{\mathbb{E}[X_2^2]}$. We substitute these estimates into the orthogonality condition (9):

$$\begin{aligned} &\mathbb{E}[(Y - X_1 \hat{a}_1 - X_2 \hat{a}_2)(X_1 - \alpha X_2)] = 0. \\ \Rightarrow &\mathbb{E}\left[(Y - X_1 \hat{a}_1 - X_2 \hat{a}_2)\left(X_1 - \frac{\mathbb{E}[X_1 X_2]}{\mathbb{E}[X_2^2]} X_2\right)\right] = 0. \\ \Rightarrow &\mathbb{E}\left[(X_1(a_1 - \hat{a}_1) + (a_2 - \hat{a}_2)X_2 + \varepsilon_3)\right. \\ &\quad \left.\left(X_1 - \frac{\mathbb{E}[X_1 X_2]}{\mathbb{E}[X_2^2]} X_2\right)\right] = 0. \\ \Rightarrow &\hat{a}_1 = a_1 \end{aligned}$$

From the above two examples it is clear that even though the internal relations between the variables are nonlinear, all we need is an unbiased linear estimate to estimate the causal parameter in a directed acyclic graph. Below we provide more general results about the recovery of the causal parameters associated with the direct causal parents of the outcome variable.

Proposition 4. Assuming a causal DAG G of variables $\{Y, \mathbf{X}\}$, where Y has no children, the noise on Y is Gaussian, the direct causal parents $\mathcal{D} := \{X_1^c, \dots, X_k^c\} \subseteq \mathbf{X}$ have a linear effect θ on the target variable Y and arbitrary nonlinear dependencies f between confounding variables $\mathcal{Z} := \mathbf{X} \setminus \mathcal{D}$ may exist, Algorithm 1 using ridge regression consistently identifies the direct causal parents of Y .

Proof. The proof is given in the Appendix. \square

Remarks on Algorithm 1: $X_i^{[j]}$ is a vector which corresponds to the samples chosen in the j^{th} subsampling procedure, $X_{\setminus i}^{[j]} = (X_1^{[j]}, \dots, X_{i-1}^{[j]}, X_{i+1}^{[j]}, \dots, X_d^{[j]})$ for any $i \in [d]$. In general the subscript i represents the estimation for the i^{th} variable and super-script j represents the j^{th} subsampling procedure. K represents the set obtained after sample splitting. $m_i^{[j]}$ and $g_i^{[j]}$ are nonlinear parametric functions to allow for nonlinear interactions among the non-output. In practice we use a z-test, implemented in (Seabold & Perktold, 2010), in all our experiments.

Algorithm 1 Efficient Causal Structure Search

```

1: Input: response  $Y \in \mathbb{R}^n$ , covariates  $\mathbb{X} \in \mathbb{R}^{n \times d}$ , significance level  $\alpha$ 
2: for Subsample  $j \in [m]$  do
3:   for  $i = 1, \dots, d$  do
4:      $D_j \leftarrow X_i^{[j]}$  and  $Z_j \leftarrow X_{\setminus i}^{[j]}$ 
5:     Fit  $m_i^{[j]}(Z_j)$  to  $D_j$ 
6:     Fit  $g_i^{[j]}(Z_j)$  to  $Y^{[j]}$ 
7:      $\hat{V}_i^{[j]} \leftarrow D_j - m_i^{[j]}(Z_j)$ 
8:      $\hat{\theta}_i^{[j]} \leftarrow \left( \frac{1}{n} \sum_{k \in K} \hat{V}_{ik}^{[j]} D_{jik} \right)^{-1} \frac{1}{n} \sum_{k \in K} \hat{V}_{ik}^{[j]} (Y_{ik}^{[j]} - g_{ik}^{[j]}(Z_j) D_{jik})$ 
9:   end for
10:  end for
11:  DecVec:=[]
12:  for  $i \in [d]$  do
13:    Gaussian normality test for the residual  $Y_i - \sum \hat{\theta}_i X_i$ 
14:    if rejected then
15:      DecVec[i] = 1
16:    else
17:      DecVec[i] = 0
18:    end if
19:  end for
20:  Return DecVec

```

4. Experiments

4.1. Partially Nonlinear Causal Discovery

We provide two concrete examples of the parameter estimation procedure using the Neyman orthogonality conditions (Neyman, 1979) for the discovery of causal parents in the partially nonlinear case. We show that using our estimation procedure we get unbiased estimates (Chernozhukov et al., 2016) of the true θ_i parameters, regardless of the highly nonlinear interactions among the covariates.

Example 1 (Figure 1) We first verify with a numerical simulation the claims regarding the example treated in Section 3.1, Figure 1, where already in the linear case ICP is unable to identify the correct causal parents (Ghassami et al., 2017) and both ICP and LRE are unable to identify the causal parent without access to the assumed interventional data (Section 2). We show that even in the case where we set $f(x) := x^2$ in equation (10), our approach is able to correctly identify the correct causal parents. Figure 3 shows the results of 50 estimation procedures, each with 1000 observations. The results are consistent with the claim in Section 3.1. A normality test (we use the z-test implemented in (Seabold & Perktold, 2010) in all our experiments) confirms that the distributions of both direct causal parents X_1 and X_2 centered around the true value, are indeed Gaussians ($p < 10^{-9}$).

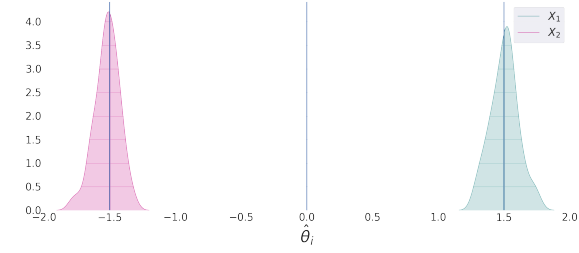


Figure 3. Estimations of the three variable case discussed 1 in Section 4.1. The true values of the θ parameters are $\theta_1 = 1.5$ and $\theta_2 = -1.5$

Example 2 (Figure 4) We then perform an experiment with the larger underlying graph shown in Figure 4, where the chosen functions for the interactions among non-output variables are $f_i(\cdot) = \tanh(\cdot)$, $\forall i$. In this example we additionally test the results of our method using a nonlinear regression technique, since Section 3.1 indicated that linear regression should be sufficient and preferred. Figure 5 shows the results of the estimation procedure.

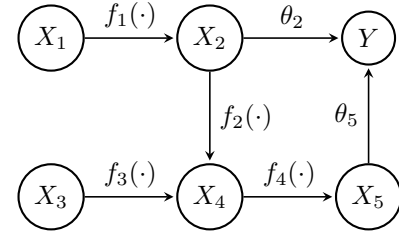


Figure 4. An example ground truth graph where all causal effects except those pointing to variable Y are given by nonlinear invertible functions $f_i(\cdot)$; effects on the output variable are linear and parametrized by θ_i .

In the version where linear regression is performed, the distributions of the estimated causal strengths θ_i (derived by regressing output Y on each variable X_i) enable to clearly identify the true causal parents, despite the nonlinear effects present in the graph. The estimate with a nonlinear regression function (Kernel Ridge regression with RBF kernel) leads to similar results. This supports the sufficiency of linear regressors described in Section 3.1.

4.2. Comparison with Invariant Causal Prediction

We compare our method with Invariant Causal Prediction (ICP) (Peters et al., 2016) over a ten variable graph ($\{X_i\}_{i=1}^9, Y$), where the output variable Y has no children, and the interactions with its parents are linear with coefficients $\theta = 5$; the graph involves ten more causal links among the covariates, which take the nonlinear functional form $f(x) = \alpha \tanh(\beta \cdot x)$, with $\alpha = 0.5$ and $\beta = 15$. Endogenous noises are assumed to be Gaussian with mean

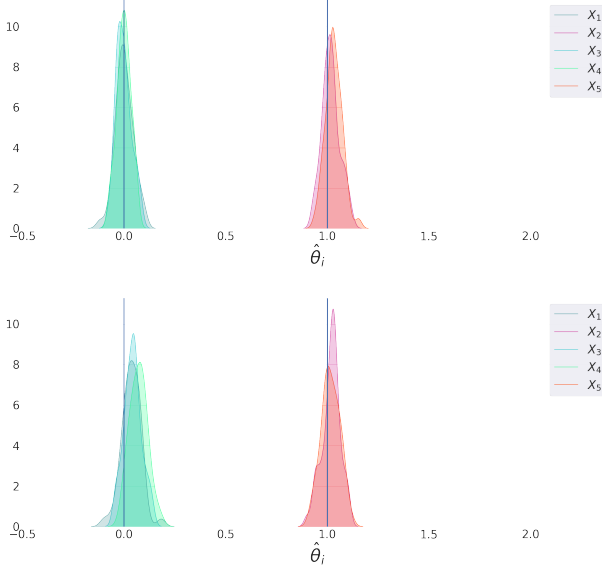


Figure 5. Distribution of the values of the $\hat{\theta}_i$ parameters across multiple estimation procedures. Figure above is estimated through a linear regression model; the two true causal parents (X_2 and X_5) have clearly distinguishable distributions, centered around the true value ($\theta_2 = \theta_5 = 1.0$), while the others are Gaussians centered around zero. The figure below reports estimates obtained through a nonlinear regression model (kernel ridge regression with a RBF kernel, $\alpha = 1.0$; (Pedregosa et al., 2011)).

0 and $\sigma = 0.3$.

The ICP based estimation result depends by construction on: 1) the number of environments; 2) the strength of the interventions. As pointed out, it is a positive feature of our approach to work as illustrated even in settings in which ICP might fail either due to lack of a sufficiently diverse set of environments or for too mild interventions or especially when only observational data is available. To show this, we compare the performance of the two methods across different cases. We vary the number of environments, strength of the interventions and overall intervened variables.

In our setting, interventions consist in setting the endogenous noise variance to $\sigma_{do} = 0.5$. The observations consist in $3 \cdot 10^5$ samples, which were split for our approach (OSS) in 150 estimation procedures performed with $2 \cdot 10^3$ observations each.

For the proposed *orthogonal structure search* (OSS), the distributions for the linear parameters of the true causal parents are easily distinguishable from those of the non-parents, see Figure 6. We decide using a z-test to check for Gaussianity of the estimated linear parameters. Our method correctly assigns a p-value of zero to the true causal parents, and identifies the other variables as non direct parents (significance threshold: 0.001).

Table 1. Comparison of p-values returned by ICP and the proposed OSS in three different experiments. Correctly identified causal parents (blue) are printed in green.

	EXP. 1		EXP. 2		EXP. 3	
	ICP	OSS	ICP	OSS	ICP	OSS
X_1	0.28	0.0	0.0	0.0	1.00	0.0
X_2	1.00	0.12	1.0	0.04	1.00	0.83
X_3	1.00	0.7	1.0	0.15	1.00	0.32
X_4	0.28	0.0	0.0	0.0	0.0	0.0
X_5	0.02	0.0	0.0	0.0	1.0	0.0
X_6	1.00	0.04	1.0	0.94	1.00	0.70
X_7	1.00	0.80	1.0	0.32	1.00	0.62
X_8	0.27	0.0	0.0	0.0	1.00	0.0
X_9	1.00	0.14	1.0	0.09	1.00	0.32

Table 1 shows the results in three different experiments. The underlying graph is the same across the three different experiments; in the first two, we perform a variety of interventions involving all of the true causal parents. In the third, we only intervene on variable X_4 . The first two differ in the nature of the interactions among the X_i variables; linear in the first case, nonlinear in the second.

ICP adopts a conservative policy, but manages to identify the true causal parents in the first two experiments. Despite not reaching the significance threshold for three of the four variables in the first experiment, it could be argued that the different nature of the variables is somehow reflected in the difference among the p-values. Interestingly, it performs well even in the presence of nonlinearities. However, in the third case, when interventions are limited, the method fails to discover all but one of the true causal variables — the only one that is intervened on in the second environment. OSS, on the other hand, is consistent across all cases, correctly identifying all of the causal parents.

Another strong difference between the two approaches is in the duration of the performed computations: in these experiments, the ICP algorithm in the R implementation¹ took ~ 230 seconds to terminate, while our own Python implementation of OSS took ~ 3 seconds. While this is not a controlled run-time study, it is encouraging that in addition to its superior scaling, our method is already faster for a relatively small (ten variable) graph.

4.3. Scaling Causal Inference to Large Graphs

In order to check the performance of the method on larger graphs, we ran an estimation procedure on 200 instances of 20 variables and 30 variables random graphs, generated

¹<https://CRAN.R-project.org/package=InvariantCausalPrediction>

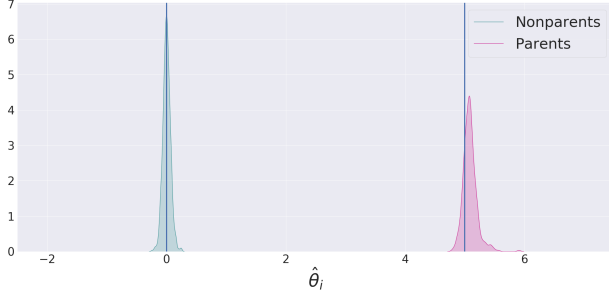


Figure 6. Distribution of the estimated θ values for the true and false causal parents in the 10 variables graph described in Section 4.2. The vertical lines indicate the ground truth values for the causal parents linear coefficients

with the Networkx package for Python (Hagberg et al., 2008). Any graph with this number of variables would require a method like Invariant Causal Prediction to check $2^{20} = 1048576$ different sets, making it a computationally expensive task. While the ICP R package provides heuristics to overcome this limitation, theoretical guarantees are lost and the performance is heavily impaired.

The ground truth causal interactions in the graph are generated as in Section 4.2. For 20 variables, the ratio between true positives and actual causal parents is 0.86, whereas the ratio false positives and actual causal parents is 0.0015.

When the dimension of the graph grows up to 30 variables, the true discovery rate is 0.67, and the ratio between false positives and actual causal parents is 0.017. The false discovery rate is therefore very small. The method is cautious in the decisions, with a very low number of false positives.

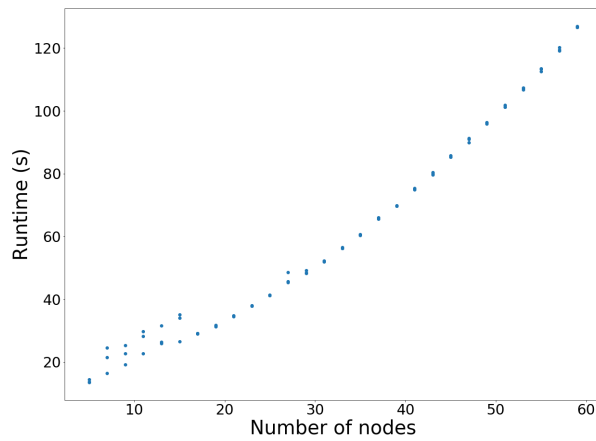


Figure 7. Runtime as a function of the number of variables.

Figure 7 shows the runtime of the method in seconds as a

function of the graph's size. Notice that the runtime of OSS on a 60 variables graph (~ 120 seconds) is still smaller than that of ICP on a 10 variables graph (~ 230 seconds).

4.4. Extension: Hidden Confounding

Table 2. p-values for variables in the hidden variable example. Correctly identified causal parents are evidenced in green, uncorrect ones in red.

	ICP	OSS
X_1	0.0	0.0
X_2	0.5	0.0

We ran an experiment on data generated using the ground truth graph in Figure 8, where the variable H is unobserved. Such a model corresponds to a misspecification of the assumptions underlying the ICP method. In such a case, the model will incorrectly identify only X_1 as a causal parent of Y (see (Peters et al., 2016), appendix C). Unless the biases in the two estimation procedures are tuned to one another in such a way that they cancel out, OSS will correctly identify a nonzero causal relationship from X_2 to Y (even though the estimate will be biased), plus a spurious causal relationship between X_1 and Y (see Appendix B for details). In this sense, the output of the method would be a superset of the true causal parents. For a toy simulation with $2.5 * 10^6$ observations and linear relationships among all variables corresponding to Figure 8, we show in Figure 10 that $\hat{\theta}_1$ converges to a nonzero quantity and $\hat{\theta}_2$ is a biased estimate of θ_2 . The p-values in Table 2 confirm empirically that a superset of ancestors and direct causal parents is returned by our algorithm.

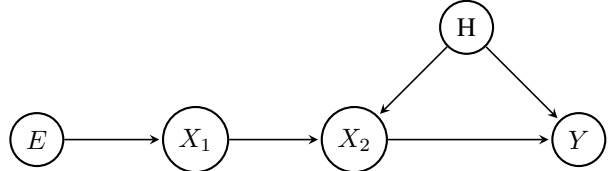


Figure 8. **Example 2** Hidden confounder, corresponding to a models misspecification for the invariance approach of invariant causal prediction (Figure 9 Peters et al., 2016, p. 45). E represent an environment in which variable X_1 is intervened on.

5. Discussion

Causal structure discovery is challenging but of high importance for many fields, especially in the presence of nonlinear relationships and/or hidden confounders. A recent empirical evaluation of different causal discovery methods highlighted the desirability of more efficient algorithms (Heinze-Deml et al., 2018). In the present work, we provide identifiability

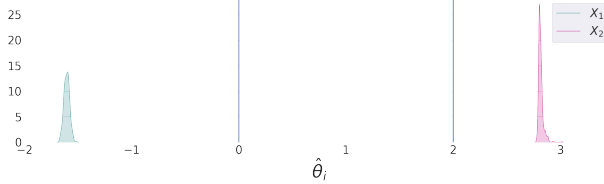


Figure 9. Simulation in case of a hidden confounder H . The estimated causal strength of X_1 converges (incorrectly) to a nonzero value, while that of X_2 is biased (see text for discussion).

results for the set of direct causal parents including the case of partially nonlinear models, as well as a highly efficient algorithm that scales linearly in the number of states and exhibits state-of-the-art performance in the reported experiments. Whilst not amounting to full causal graph discovery, identification of causal parents is of major interest in real-world applications, e.g., when assaying the causal influence of genes on the phenotype, or in system identification for robotics.

Acknowledgements

We thank Nicolai Meinshausen and Victor Chernozhukov for helpful discussions. This research was partially supported by the Max Planck ETH Center for Learning Systems.

References

Caponnetto, A. and De Vito, E. Optimal rates for the regularized least-squares algorithm. *Foundations of Computational Mathematics*, 7(3):331–368, 2007.

Chernozhukov, V., Chetverikov, D., Demirer, M., Duflo, E., Hansen, C., and Newey, W. K. Double machine learning for treatment and causal parameters. Technical report, cemmap working paper, Centre for Microdata Methods and Practice, 2016.

Christiansen, R. and Peters, J. Switching regression models and causal inference in the presence of latent variables. *arXiv preprint arXiv:1808.05541*, 2018.

Ghassami, A., Salehkaleybar, S., Kiyavash, N., and Zhang, K. Learning causal structures using regression invariance. In *Advances in Neural Information Processing Systems*, pp. 3011–3021, 2017.

Gretton, A., Fukumizu, K., Harchaoui, Z., and Sriperumbudur, B. K. A fast, consistent kernel two-sample test. In *Advances in neural information processing systems*, pp. 673–681, 2009.

Hagberg, A. A., Schult, D. A., and Swart, P. J. Exploring network structure, dynamics, and function using networkx. In Varoquaux, G., Vaught, T., and Millman, J. (eds.), *Proceedings of the 7th Python in Science Conference*, pp. 11 – 15, Pasadena, CA USA, 2008.

Heinze-Deml, C., Maathuis, M. H., and Meinshausen, N. Causal structure learning. *Annual Review of Statistics and Its Application*, 5:371–391, 2018.

Hoyer, P. O., Janzing, D., Mooij, J. M., Peters, J., and Schölkopf, B. Nonlinear causal discovery with additive noise models. In *Advances in neural information processing systems*, pp. 689–696, 2009.

Javanmard, A. and Montanari, A. De-biasing the lasso: Optimal sample size for gaussian designs. arxiv, 2015.

Maathuis, M. H., Colombo, D., Kalisch, M., and Bühlmann, P. Predicting causal effects in large-scale systems from observational data. *Nature Methods*, 7(4):247, 2010.

Mooij, J., Janzing, D., Peters, J., and Schölkopf, B. Regression by dependence minimization and its application to causal inference in additive noise models. In *Proceedings of the 26th annual international conference on machine learning*, pp. 745–752. ACM, 2009.

Mooij, J., Janzing, D., Schölkopf, B., and Heskes, T. On Causal Discovery with Cyclic Additive Noise Models. In Shawe-Taylor, J., Zemel, R., Bartlett, P., Pereira, F., and Weinberger, K. (eds.), *Advances in Neural Information Processing Systems 24*, pp. 639–647, Red Hook, NY, USA, 2011. Curran Associates, Inc.

Neyman, J. C (α) tests and their use. *Sankhyā: The Indian Journal of Statistics, Series A*, pp. 1–21, 1979.

Nichols, A. Causal inference with observational data. *The Stata Journal*, 7(4):507–541, 2008.

Pearl, J. *Causality*. Cambridge university press, 2009.

Pedregosa, F., Varoquaux, G., Gramfort, A., Michel, V., Thirion, B., Grisel, O., Blondel, M., Prettenhofer, P., Weiss, R., Dubourg, V., Vanderplas, J., Passos, A., Cournapeau, D., Brucher, M., Perrot, M., and Duchesnay, E. Scikit-learn: Machine learning in Python. *Journal of Machine Learning Research*, 12:2825–2830, 2011.

Peters, J., Mooij, J. M., Janzing, D., and Schölkopf, B. Identifiability of causal graphs using functional models. In *Proceedings of the 27th Annual Conference on Uncertainty in Artificial Intelligence (UAI)*, pp. 589–598, 2011.

Peters, J., Mooij, J. M., Janzing, D., and Schölkopf, B. Causal discovery with continuous additive noise models. *The Journal of Machine Learning Research*, 15(1):2009–2053, 2014.

Peters, J., Bühlmann, P., and Meinshausen, N. Causal inference by using invariant prediction: identification and confidence intervals. *Journal of the Royal Statistical Society: Series B (Statistical Methodology)*, 78(5):947–1012, 2016.

Peters, J., Janzing, D., and Schölkopf, B. *Elements of causal inference: foundations and learning algorithms*. MIT press, 2017.

Pfister, N., Bauer, S., and Peters, J. Identifying causal structure in large-scale kinetic systems. *arXiv preprint arXiv:1810.11776*, 2018a.

Pfister, N., Bühlmann, P., and Peters, J. Invariant causal prediction for sequential data. *Journal of the American Statistical Association*, 2018b.

Rothenhäusler, D., Bühlmann, P., Meinshausen, N., and Peters, J. Anchor regression: heterogeneous data meets causality. *arXiv preprint arXiv:1801.06229*, 2018.

Seabold, S. and Perktold, J. Statsmodels: Econometric and statistical modeling with python. In *9th Python in Science Conference*, 2010.

Shimizu, S., Hoyer, P. O., Hyvärinen, A., and Kerminen, A. A linear non-gaussian acyclic model for causal discovery. *Journal of Machine Learning Research*, 7(Oct):2003–2030, 2006.

Slutsky, E. Über stochastische asymptoten und grenzwerte. *Metron*, 5(3):3–89, 1925.

Spirites, P., Glymour, C. N., Scheines, R., Heckerman, D.,
Meek, C., Cooper, G., and Richardson, T. *Causation,
prediction, and search*. MIT press, 2000.

Appendix

A. Causal Discovery via Orthogonalization

Proof of Example 2. Let us start from the easier case first. Let us first try to estimate the coefficient of interaction between X_2 and X_3 but it is also very clear that the estimation of a_{23} will be unbiased as the given setting precisely match with the double machine learning setting. However, we will see in this example that given the population, a_{13} can be approximated as well. Let us write down the structural equation model first:

$$\begin{aligned} X_3 &:= a_{13}X_1 + a_{23}X_2 + \varepsilon_3 \\ X_2 &:= a_{12}X_1 + \varepsilon_2 \\ X_1 &:= \varepsilon_1 \end{aligned} \tag{11}$$

From the set of equations we have:

$$X_1 = a_{12}^{-1}X_2 - a_{12}^{-1}\varepsilon_2$$

Let also denote $\mathbb{E}[\varepsilon_1^2] = \sigma_1^2$ and $\mathbb{E}[\varepsilon_2^2] = \sigma_2^2$. Hence, $\mathbb{E}[X_1^2] = \sigma_1^2$, $\mathbb{E}[X_1X_2] = a_{12}\sigma_1^2$ and $\mathbb{E}[X_2^2] = a_{12}\mathbb{E}[X_1X_2] + \mathbb{E}[\varepsilon_2X_2] = a_{12}^2\sigma_1^2 + \sigma_2^2$. Let us first try to find the regression coefficient of fitting X_2 on X_3 .

$$X_3 = \hat{a}_{23}X_2 + \eta_1$$

Hence, $\hat{a}_{23} = \frac{\mathbb{E}[X_2X_3]}{\mathbb{E}[X_2^2]}$ if η is independent of X_2 .

$$\hat{a}_{23} = \frac{\mathbb{E}[X_2X_3]}{\mathbb{E}[X_2^2]} = \frac{\mathbb{E}[X_2(a_{13}X_1 + a_{23}X_2 + \varepsilon_3)]}{\mathbb{E}[X_2^2]} = a_{23} + a_{13}a_{12}\frac{\sigma_1^2}{\sigma_2^2 + a_{12}^2\sigma_1^2} \tag{12}$$

Similarly, if we fit X_2 on X_1 then

$$X_1 = \hat{a}_{12}^{-1}X_2 + \eta_2$$

then $\hat{a}_{12}^{-1} = \frac{\mathbb{E}[X_1X_2]}{\mathbb{E}[X_2^2]}$. However $\mathbb{E}[X_1X_2]$ can also be written as following:

$$\mathbb{E}[X_1X_2] = a_{12}^{-1}\mathbb{E}[X_2^2] - a_{12}^{-1}\mathbb{E}[\varepsilon_2X_2]$$

Hence,

$$\hat{a}_{12}^{-1} = a_{12}^{-1} \left(1 - \frac{\sigma_2^2}{\sigma_2^2 + a_{12}^2\sigma_1^2} \right) = a_{12}^{-1} \left(\frac{a_{12}^2\sigma_1^2}{\sigma_2^2 + a_{12}^2\sigma_1^2} \right)$$

Residual $\hat{V} = X_1 - \hat{a}_{12}^{-1}X_2$. Hence we can have

$$\mathbb{E}(\hat{V}X_1) = \mathbb{E}[X_1^2] - \hat{a}_{12}^{-1}\mathbb{E}[X_1X_2] = \mathbb{E}[\varepsilon_1^2] - \hat{a}_{12}^{-1}a_{12}\mathbb{E}[\varepsilon_1^2] = \frac{\sigma_1^2\sigma_2^2}{\sigma_2^2 + a_{12}^2\sigma_1^2}$$

We now calculate,

$$\begin{aligned} \mathbb{E}[\hat{V}(X_3 - \hat{a}_{23}X_2)] &= \mathbb{E}[(X_1 - \hat{a}_{12}^{-1}X_2)(X_3 - \hat{a}_{23}X_2)] \\ &= \mathbb{E}[(X_1 - \hat{a}_{12}^{-1}X_2)((a_{23} - \hat{a}_{23})X_2 + a_{13}X_1 + \varepsilon_3)] \\ &= (a_{23} - \hat{a}_{23})a_{12}\sigma_1^2 + a_{13}\sigma_1^2 - \hat{a}_{12}^{-1}(a_{23} - \hat{a}_{23})(\sigma_2^2 + a_{12}^2\sigma_1^2) - \hat{a}_{12}^{-1}a_{13}a_{12}\sigma_1^2 \\ &= \frac{a_{13}\sigma_1^2\sigma_2^2}{\sigma_2^2 + a_{12}^2\sigma_1^2} \end{aligned}$$

Last equation was written after step of minor calculation. Since the estimator is

$$\hat{a}_{13} = \left[\mathbb{E}(\hat{V}X_1) \right]^{-1} \mathbb{E}[\hat{V}(X_3 - \hat{a}_{23}X_2)] = a_{13}$$

□

Proof of Lemma 3. Using the Markov factorization

$$P(\mathbf{W}; \theta, \boldsymbol{\eta}) = P(Y|\mathbf{Z}, X_K; \theta, \boldsymbol{\beta})P(\mathbf{Z}, X_K; \boldsymbol{\gamma})$$

due to linearity and gaussianity of the assignement of Y , we obtain a negative log likelihood of the form (up to additive constants)

$$\ell(\mathbf{W}; \theta, \boldsymbol{\eta}) = \frac{1}{2\sigma_Y^2} (Y - X_k \theta - \mathbf{Z}^\top \boldsymbol{\beta})(Y - X_k \theta - \mathbf{Z}^\top \boldsymbol{\beta}) + f(X_k, \mathbf{Z}; \boldsymbol{\gamma})$$

where f stands for the negative log likelihood of the second factor. Following Chernozhukov et al. (2016)[eq. (2.7)], this leads to the Neyman orthogonal score

$$\psi(\mathbf{W}; \theta, \boldsymbol{\eta}) = \partial_\theta \ell(\mathbf{W}; (\theta, \boldsymbol{\eta})) - \boldsymbol{\mu} \partial_\eta \ell(\mathbf{W}; (\theta, \boldsymbol{\eta})) = -\frac{1}{\sigma_Y^2} (Y - X_k \theta - \mathbf{Z}^\top \boldsymbol{\beta}) X_k - \boldsymbol{\mu} \left(-\frac{1}{\sigma_Y^2} (Y - X_k \theta - \mathbf{Z}^\top \boldsymbol{\beta}) \mathbf{Z} + \partial_\gamma f(X_k, \mathbf{Z}; \boldsymbol{\gamma}) \right)$$

Following eq. (2.8) of the same paper, we derive the expression of $\boldsymbol{\mu}$ as

$$\boldsymbol{\mu} = J_{\theta, \eta} J_{\eta, \eta}^{-1}$$

with

$$J_{\eta, \eta} = \partial_{\eta^\top} \mathbb{E} [\partial_\eta \ell(\mathbf{W}, \theta, \boldsymbol{\eta})] = \begin{bmatrix} \sigma_Y^{-2} \mathbb{E} [Z^\top Z] & \mathbf{0} \\ \mathbf{0} & \partial_{\gamma^\top} \mathbb{E} [\partial_\gamma f(X_k, Z; \boldsymbol{\gamma})] \end{bmatrix},$$

and

$$J_{\theta, \eta} = \partial_{\eta^\top} \mathbb{E} [\partial_\theta \ell(\mathbf{W}, \theta, \boldsymbol{\eta})] = \sigma_Y^{-2} \begin{bmatrix} \mathbb{E} [X_k^\top Z] & \mathbf{0} \end{bmatrix},$$

resulting in

$$\boldsymbol{\mu} = \mathbb{E} [X_k^\top Z] \mathbb{E} [Z^\top Z]^{-1}$$

Reintroducing $\boldsymbol{\mu}$ in the expression of ψ leads to the result. \square

Proof of Proposition 4. We can first try to show what happens if we use an unbiased estimator. Similar to the example discussed before with three variable case we can try to write the population version of the estimates. The Neyman orthogonality conditions is following:

$$\mathbb{E}[(Y - D\hat{\theta} - X\hat{\beta})(D - X\beta)]^2 = 0 \quad (13)$$

Now similar to the simple three variable case, we assume that we do want to model $Y = \beta \mathbf{X} + \eta$. Hence, $\beta = [\mathbb{E}[X^\top X]]^{-1} \mathbb{E}[X^\top Y]$. We can also get unbiased linear coefficient for $\hat{\alpha} = [\mathbb{E}[X^\top X]]^{-1} \mathbb{E}[X_1^\top X_2]$. We can put these estimates in the Neyman orthogonal scores to satisfy and we can easily see that the estimate $\hat{\theta} = \theta$. However, we do use ridge regression which is biased but again our Neyman orthogonal score is same as in the paper (Chernozhukov et al., 2016) hence under the assumption from double ML, we would have $\sqrt{n}(\hat{\theta} - \theta) \rightarrow \mathcal{N}(0, \Sigma)$ where Σ is a covariance matrix (Theorem 4.1 (Chernozhukov et al., 2016)).

Now we have at-least one test which is exponential in time but is asymptotically consistent and can be used for detecting significant causal parents from the non-causal parents. Let us assume that the set \hat{Z} consists of all the variable. Get all the possible decomposition of the set into two disjoint set and then test for the residual of Y . Following from the Slutsky theorem (Slutsky, 1925), only one of the cases would follow asymptotic normal decomposition:

$$Y_i - \sum \hat{\theta}_i X_i \sim \mathcal{N}(0, \Sigma) \quad (14)$$

for some arbitrary Σ , which in practice we normalize to be 1. Using any consistent two-sample test (Gretton et al., 2009) and test statistics V , we have: $\hat{V}_{k,l}(X'_{\dots N}, \hat{E}'_{\dots N}) \xrightarrow{P} V_{k,l}(X, E)$ for $N \rightarrow \infty$.

The consistency of the algorithm then follows from the consistency of ridge regression (Caponnetto & De Vito, 2007). \square

B. Biased estimates in the case of a hidden confounder

Consider the graph in figure 10, and linear relationships among the variables. This yields the SEM

$$\begin{aligned}
 Y &:= X_1\theta_1 + X_2\theta_2 + \varepsilon_Y \\
 X_2 &:= X_0\beta_0 + X_1\beta_1 + \varepsilon_2 \\
 X_1 &:= \varepsilon_1 \\
 X_0 &:= \varepsilon_0
 \end{aligned} \tag{15}$$

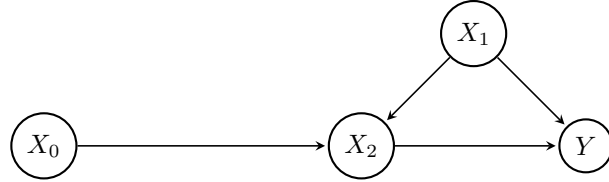


Figure 10. Hidden confounder: variables X_0 , X_2 , and Y are observed, while variable X_1 is hidden.

Applying our causal discovery algorithm will require us to iteratively construct estimates of θ_0 and θ_2 (the former being, in our case, 0). The Neyman orthogonality condition for the estimator $\hat{\theta}_2$ reads:

$$\mathbb{E} \left[\left(Y - X_2\hat{\theta}_2 - X_0\hat{\beta}_0 \right) \left(X_2 - X_0 \frac{\mathbb{E}[X_2X_0]}{\mathbb{E}[X_0^2]} \right) \right] = 0 \tag{16}$$

We can compute the left hand side, and it reads

$$\begin{aligned}
 &\mathbb{E} \left[\left(Y - X_2\hat{\theta}_2 - X_0\hat{\beta}_0 \right) \left(X_2 - X_0 \frac{\mathbb{E}[X_2X_0]}{\mathbb{E}[X_0^2]} \right) \right] = \\
 &\mathbb{E} \left[\left(X_1\theta_1 + X_2\theta_2 - X_2\hat{\theta}_2 - X_0\hat{\beta}_0 \right) \left(X_0\beta_0 + X_1\beta_1 + \varepsilon_2 - X_0 \frac{\mathbb{E}[X_2X_0]}{\mathbb{E}[X_0^2]} \right) \right]
 \end{aligned}$$

Collecting all the terms and simplifying, the equation reads

$$\theta_2 - \hat{\theta}_2 = \frac{\mathbb{E}[(X_1\theta_1)^2]}{\mathbb{E}[X_1\beta_1] + \sigma_2^2} \tag{17}$$

A nonzero bias will likewise show up when computing the Neyman orthogonality condition for $\hat{\theta}_0$, which in reality should be zero. We have then shown is that a nonzero bias in the estimate will remain due to hidden, unobserved confounder; hence $\{\hat{\theta}_i\}_{i=0,2}$ will both be biased; in particular, $\hat{\theta}_0$ will in general be nonzero.